Neoplasma 2023; 70(6): 747–760

doi:10.4149/neo_2023_230125N41

Tumor-derived autophagosome vaccines combined with immune adjuvants mediate antitumor immune responses via the neoantigen pathway

Jia YUAN[1], Yue CHANG[2], Yalan DAI[2], Yutong CHEN[2], Rongbin YUE[3], Linjuan ZENG[2,*]

[1]Department of Oncology, Jiangmen Central Hospital, Affiliated Jiangmen Hospital of Sun Yat-sen University, Jiangmen, China; [2]Department of Abdominal Oncology, The Cancer Center of the Fifth Affiliated Hospital of Sun Yat-sen University, Zhuhai, China; [3]Department of Hepatobiliary Surgery, The Fifth Affiliated Hospital of Sun Yat-sen University, Zhuhai, China

**Correspondence: zenglinj@mail.sysu.edu.cn*

Received January 25, 2023 / Accepted November 23, 2023

Vaccines composed of autophagosomes derived from tumor cells called DRibbles (DRiPs-containing blebs) are involved in the cross-presentation of tumor antigens, thus inducing cross-reactive T-cell responses against the tumor. Compared with traditional tumor lysate vaccines, autophagosome vaccines were found to be better sources of multiple tumor-associated antigens (TAAs) that activate antigen-specific T-cells. However, the involvement of tumor neoantigens in the immune responses of autophagosome vaccines remains unclear. The present study showed that exogenous autophagosome vaccines (DRibbles) combined with immune adjuvants (anti-OX40 antibody and ATP) can effectively activate functional T cells *in vitro*. Importantly, the combination of exogenous tumor-derived autophagosome vaccines and immune adjuvants was found to induce tumor regression in B16F10 and 4T1 tumor-bearing mice. The combination of autophagosome-enriched DRibbles with anti-OX40 antibody and ATP also exhibited optimal immune stimulation and antitumor efficiency *in vivo*. The effectiveness of exogenous DRibble vaccines was mainly due to their enhancement of tumor immunogenicity by increasing the presentation and release of tumor neoantigens. These findings suggest that this immunotherapeutic method may be effective in the treatment of cancer.

Key words: DRibble vaccines; anti-OX40 antibody; ATP; neoantigen; immunotherapy

Malignant tumors are one of the top three causes of death worldwide, they seriously affect human health and pose a threat to survival [1]. In addition to traditional treatments, such as surgery, radiotherapy, and chemotherapy, immunotherapy is increasingly used to treat cancer patients [2]. Cancer vaccines are important in immunotherapy but their clinical efficacy is often limited by their low immunogenicity, which is not sufficient to stimulate cellular immune responses. Optimization of the design of cancer vaccines requires the development and selection of better adjuvants and transport carriers and the determination of optimal dosages, routes of administration, period, and frequency [3–5]. Tumor immunogenicity may be enhanced and the tumor immunosuppressive microenvironment improved by combining cancer vaccines with other immunotherapy regimens, chemoradiotherapy, and other anti-tumor agents, thus increasing the efficacy of treatment and expanding therapeutic indications [6, 7].

Autophagy plays an important role in processing cell proteins. During this process, damaged cytosolic proteins or organelles are enclosed in autophagosomes and delivered to lysosomes for recycling or clearance [8, 9]. Autophagy also plays vital roles in both innate and adaptive immunity [10]. The induction of tumor cell autophagy and the inhibition of lysosomal activity can result in autophagosome wrapping of a broad spectrum of tumor antigens, including defective ribosomal products (DRiPs) and both long-lived and short-lived proteins. These autophagosome-enriched DRiP-containing blebs have been named DRibbles [11, 12]. Co-administration of co-stimulatory antibodies, such as anti-OX40 (CD134), has been found to enhance DRibble-induced T-cell expansion. Anti-OX40 co-stimulatory antibody could directly influence the expansion of effector T-cells and the inhibition of Tregs. DRibble vaccines combined with an anti-OX40 antibody were found to significantly enhance T-cell priming and anti-tumor activity [13, 14].

Copyright © 2023 The Authors.
This article is licensed under a Creative Commons Attribution 4.0 International License, which permits use, sharing, adaptation, distribution, and reproduction in any medium or format, as long as you give appropriate credit to the original author(s) and the source and provide a link to the Creative Commons licence. To view a copy of this license, visit https://creativecommons.org/licenses/by/4.0/

Adenosine triphosphate (ATP) is an important signaling molecule that has been shown to attract dendritic cells (DCs), promote their maturation, improve their uptake of antigens, and enhance their homing to lymph nodes. In addition, ATP can directly affect Tregs and MDSCs to eliminate immune suppression. Vaccines composed of nanoparticles with adjuvant ATP have been found to stimulate strong anti-tumor cell immunity, making ATP a new and effective vaccine adjuvant [15]. Therefore, ATP might expand the antitumor immune responses of DRibble vaccines by both enhancing tumor antigen presentation and immune cell recruitment [16–18].

Next-generation sequencing technology has shown that neoantigen vaccines could promote the development of precision medicine [19, 20]. This process, however, has drawbacks, including sample errors, tumor heterogeneity, low predictive accuracy, and high cost, limiting the personalized identification, verification, and effectiveness of neoantigen vaccines [21]. DRibbles preserve many tumor antigens, including both short-lived and long-lived proteins and incomplete ribosome products. DRibble cancer vaccines have the potential ability to target hidden tumor antigen epitopes and enhance T cell immunity, suggesting that DRibbles may serve as potential alternatives to large-scale sequencing in the search for new epitopes [22–25].

Although DRibbles contain shared tumor-associated antigens, less is known about whether autophagosome cancer vaccines contain unique tumor neoantigens. Moreover, the specific effectiveness of DRibble vaccines has not been compared with the effectiveness of other tumor vaccines. The present study showed that exogenous autophagosome vaccines contain important neoantigens that can activate large numbers of tumor-specific T-cells, with these vaccines having greater antigenic activity than ordinary tumor lysate vaccines. Moreover, the present study found that DRibble vaccines combined with immune adjuvants (anti-OX40 antibody and ATP) can effectively mediate tumor regression *in vivo*. Taken together, these findings show that autophagosome-enriched DRibbles can enhance tumor immunogenicity by releasing tumor neoantigens, suggesting that these DRibbles may be effective in the treatment of cancer.

Materials and methods

Reagents. Rapamycin (Sigma, St. Louis, MO, USA) was dissolved in DMSO and diluted with RPMI medium. Anti-OX40 antibody (119415, Peprotech, Cranbury, NJ, USA), ATP (Sigma), bortezomib (MCE, Monmouth Junction, NJ, USA), and NH_4Cl (Sigma) were dissolved in PBS and diluted with RPMI medium. PMA/Ionomycin (P/I) was purchased from Sigma. The long peptides for immunogenic B16F10 and 4T1 mutations were synthesized by Sangon Biotech (Shanghai, China). Antibodies to LC3B (12513S) and GAPDH (2118L) were purchased from Cell Signaling, Danvers, MA USA. Antibodies used for immunohistochemistry assays included anti-mouse CD3 (ab23926), anti-mouse CD4 (ab33779), anti-mouse CD8 (ab36578), and anti-mouse FOXP3 (ab96048) from Abcam, Cambridge, UK. Antibodies used for flow cytometry assay included anti-mouse CD16/32 mAb (101301, BD Biosciences, USA), anti-mouse CD3-PEcy5 (155619), anti-mouse CD4-FITC (116004), anti-mouse CD8-FITC (155004), anti-mouse IFN-γ-APC (505860), anti-mouse TNF-α-PE (506306), and anti-mouse FOXP3-PE (126404) from BioLegend, San Diego, CA, USA.

Preparation of autophagosome-enriched DRibbles and tumor cell lysate protein. Autophagosome-enriched DRibbles were prepared as described previously [12]. Briefly, B16F10 and 4T1 cells were treated with rapamycin (25 nM), bortezomib (100 nM), and NH_4Cl (10 mM) for 24–48 h. The resulting suspension was separated into the autophagosome-containing large vesicles (DRibbles). Tumor cell lysate proteins were prepared by subjecting cells to five freeze-thaw cycles of incubation at –80 °C for 30 min and 37 °C for 3 min, with an oscillation of 1 min. Protein concentrations were determined using BCA protein assay kits (Thermo Fisher Scientific, USA). Samples were stored in PBS for up to 1 month at –20 °C and for longer at –80 °C.

LC3 immunofluorescence assay. B16F10 and 4T1 cells were treated with vehicle or rapamycin (25 nM), bortezomib (100 nM), and NH_4Cl (10 mM) for 8–12 h. Then, the cells were fixed in cold absolute methanol and blocked with 1% BSA in PBST buffer (PBS plus 0.1% Tween 20) for one hour and incubated with the primary antibody against LC3B overnight at 4 °C. Subsequently, the cells were incubated with a fluorochrome-conjugated secondary antibody diluted in a blocking buffer for one hour at 37 °C in the dark. The stained samples finally were mounted in Prolong Diamond Antifade with DAPI (Invitrogen, USA). Fluorescence images were collected and processed using ImageJ software.

Autophagosome ultrastructure assay. The autophagosomes of B16F10 or 4T1 cells were directly observed and identified by transmission electron microscopy. B16F10 and 4T1 cells were fixed and embedded. The thin sections (90 nm) were observed under a JEOL 1200EX transmission electron microscope at 80 kV. The typical double-membrane vacuoles (0.1–1.0 μm) could be defined as autophagosomes.

Western blotting assay. Quantified autophagosome-enriched DRibbles and tumor cell lysate proteins prepared from B16F10 or 4T1 cells were loaded onto SDS-PAGE and transferred to PVDF membranes. LC3 (1:1000) and GAPDH (1:1000) were the primary antibodies. Primary antibodies were incubated overnight at 4 °C, then washed, and the secondary HRP-conjugated antibody was applied. The immunoreactive bands were observed with chemiluminescent substrates.

Mouse models and *in vivo* vaccination. BALB/c and C57BL/6 mice were purchased from Guangdong Animal Center (Guangzhou, China) and housed in a specific pathogen-free environment at the Experimental Animal

Center of Jinan University. Animal experiments were conducted at Jinan University (Guangzhou, China), according to the guidelines of the Jinan University Experimental Animal Center. All animal experiments were approved by the Ethics Committee of Jinan University (approval number: IACUC-20190916-07).

Melanomas were established in female C57BL/6 mice aged 6–8 weeks by subcutaneous implantation of 5×10^4 B16F10 cells each on the left and the right sides of the abdomen. Five days later, the mice were randomly distributed into various groups and vaccinated with B16F10-DRibble vaccines (20 μg), with or without anti-OX40 antibody (60 μg) and ATP (200 μg), by injection into bilateral inguinal lymph nodes. DRibble-loaded DCs (20 μg/3 million) with or without anti-OX40 antibody (60 μg) and ATP (200 μg) were injected subcutaneously into the abdomen on days 7 and 10.

Breast carcinomas were established in female BALB/c mice aged 6–8 weeks by subcutaneous implantation of 2×10^5 4T1 cells each on the left and the right sides of the abdomen. Seven days later, the mice were randomly distributed into various groups and vaccinated with 4T1-DRibble vaccines (20 μg), with or without anti-OX40 antibody (60 μg) and ATP (200 μg), by injection into bilateral inguinal lymph nodes. DRibble-loaded DCs (20 μg/3 million) with or without anti-OX40 antibody (60 μg) and ATP (200 μg) were injected subcutaneously into the abdomen on days 9 and 12.

Tumor sizes were measured every 2–3 days using calipers. Tumor volume was calculated using the formula $(A\times B^2)\times0.5$, where A was the largest and B was the smallest tumor diameter. The mice were sacrificed when the largest tumor diameter reached 2 cm or they reached a humane endpoint (obviously thin or weak).

***In vitro* generation of mature bone marrow-derived dendritic cells (BMDCs) and mixed lymphocyte reaction (MLR).** Bone marrow cells were obtained from tibias and femurs of healthy female C57BL/6 and BALB/c mice aged 6–8 weeks. Then cells were passed through 40 μm cell strainers (BD Falcon). After centrifugation at 200×g for 3 min, red blood cells (RBCs) were lysed with ACK lysis buffer (BioLegend) for 10 min. The collected cells were then planted in six-well plates at a density of 1×10^6 cells/ml in RPMI 1640 medium added with 10% fetal bovine serum (FBS), 20 ng/ml mouse granulocyte macrophage colony-stimulating factor (GM-CSF) (Peprotech), 10 ng/ml mouse IL-4 (Peprotech), and 50 μM β-mercaptoethanol (Sigma). Every three days, half of the medium with the same amount of fresh medium containing cytokines was replaced. Seven days after initial planting, the harvested non- and semi-adherent cells were regarded as mature BMDCs and were loaded with B16F10/4T1 cell-derived DRibbles (20 μg/ml) or long peptides (20 μg/ml) for 48 h.

Spleens were harvested from C57BL/6 and BALB/c mice inoculated with vaccines under sterile conditions. Then splenocytes were isolated by 40 μm cell strainers as response cells. Mixing splenocytes with the antigen-loaded mature BMDCs (10:1). The cell clusters were observed and imaged under a light microscope (CKX31, OLYMPUS, Japan) after 3–4 days of incubation.

IFN-γ ELISpot assay. Approximately 5×10^5 splenocytes were added to each cell of an anti-IFN-γ coated multiscreen 96-well plate. Mature BMDCs loaded with DRibbles (20 μg/ml) or peptides (20 μg/ml) were added. Cells treated with 500 ng/ml PMA and 1 μg/ml ionomycin were the positive controls. The cells were incubated at 37 °C for 12–16 h and the concentration of IFN-γ in the medium was measured using an anti-IFN-γ antibody ELISpot kit (DAKEWE, Shenzhen), along with an ELISpot analyzer and ImmunoSpot Professional Software (CTL–ImmunoSpot®S6 FluoroSpot, USA).

Flow cytometry. Single-cell specimens were pre-incubated with anti-CD16/32 mAb at 4 °C for 15 min and incubated at 4 °C for 30 min with various combinations of fluorochrome-conjugated antibodies, including PEcy5-conjugated anti-CD3, FITC-conjugated anti-CD4, and FITC-conjugated anti-CD8 antibodies. For intracellular cytokine staining, mouse immune cells were restimulated with antigen-loaded DCs in complete RPMI 1640 media containing 50 IU/ml recombinant IL-2 (Peprotech) at 37 °C for 1 h, followed by incubation with 1× GolgiStop and 1× GolgiPlug (BD Biosciences, USA) at 37 °C for 4–8 h. The cells were permeabilized using a Fixation and Permeabilization Kit (BD, USA) and incubated with APC-conjugated anti-IFN-γ, PE-conjugated anti-TNF-α, and PE-conjugated anti-FOXP3 antibodies. The cells were sorted by flow cytometry (FASC Canto II, BD, USA), with the data analyzed by BD FACSDiva and FlowJo software (version 10.4).

Immunohistochemistry (IHC). Tumor tissue samples were fixed with 4% paraformaldehyde and incubated with anti-CD3, anti-CD4, anti-CD8, and anti-FOXP3 antibodies. The samples were monitored and photographed using a light microscope. Areas positive for CD4, CD8, and FOXP3 were quantified within manually pre-defined tumor regions by computerized image analysis using Imagine J software.

Data mining from public databases. The Tumor IMmune Estimation Resource (TIMER) database is a comprehensive resource that automatically analyzes associations between immune infiltration levels and a series of variables (https://cistrome.shinyapps.io/timer/). The database was used to explore the correlation between ATG8/12 expression and the abundance of CD4+ T cells, CD8+ T cells, and DCs in breast invasive carcinoma (BRCA) and skin cutaneous melanoma (SKCM) tissues.

Statistical analysis. Experiments were independently repeated at least three times. All results were expressed as means ± standard deviations (SD). Statistically significant differences among individual treatments and the corresponding control groups were analyzed by Student's t-test or analysis of variance (ANOVA) test. Survival was evaluated by the Kaplan-Meier method and compared by log-rank tests. All statistical analyses were performed using GraphPad

Prism 5 software, with p-values less than 0.05 considered statistically significant.

Results

Induction of autophagosomes in B16F10 and 4T1 cells. Treatment of cells with the autophagy inducer rapamycin, the proteasome inhibitor bortezomib, and the lysosomal inhibitor NH_4Cl induced the production of large numbers of autophagosomes, which accumulated in these cells and were secreted into the culture media. These autophagosome-containing large vesicles (DRibbles) contained a broad range of antigens capable of priming an extensive repertoire of T cells [12]. Immunofluorescence staining showed that the level of expression of the autophagy-specific marker LC3B was higher in B16F10 and 4T1 cells treated with rapamycin, bortezomib, and NH_4Cl than in control cells in a normal medium (Figure 1A). Electron microscopy showed that many of these cells contained large numbers of autophagosomes/autolysosomes with the typical double-membrane structure and differential light density (Figure 1B). Western blotting showed that the expression of LC3-II/LC3-I was significantly higher in DRibbles than in cell lysates of untreated B16F10 or 4T1 cells, with the ratio of LC3-II to LC3-I proportional to the level of autophagy (Figures 1C, 1D). Taken together, these findings demonstrated that the treatment of B16F10 and 4T1 cells with an autophagy inducer, a proteasome inhibitor, and a lysosomal inhibitor generated large numbers of autophagosome-enriched DRibbles.

B16F10/4T1-derived autophagosome-enriched DRibbles combined with immune adjuvants efficiently activated T-cells *in vitro*. During immune responses, ATP can act as an important signal for antigen-presenting cells and can stimulate the tumor infiltration of cytotoxic T lymphocytes [16]. Furthermore, the combination of autophagosome-enriched DRibbles and anti-OX40 antibody was found to efficiently enhance immune responses [13]. To further investigate whether the addition of ATP could enhance the efficacy of DRibble vaccines, an appropriate concentration of ATP (250 nM) was added to the cell medium to mimic the effects of chemotherapeutic agents and other stress conditions that induce ATP release. The aggregation of splenic T-cells incubated with vehicle or with B16F10/4T1-derived DRibbles (20 μg/ml) and the immune adjuvants anti-OX40 antibody (10 μg/ml) and ATP (250 nM) were monitored by light microscopy. Incubation of these three reagents resulted in a greater aggregation of splenic T-cells (Figure 2A) and a greater activation of T-cells (Figures 2B, 2C) than did

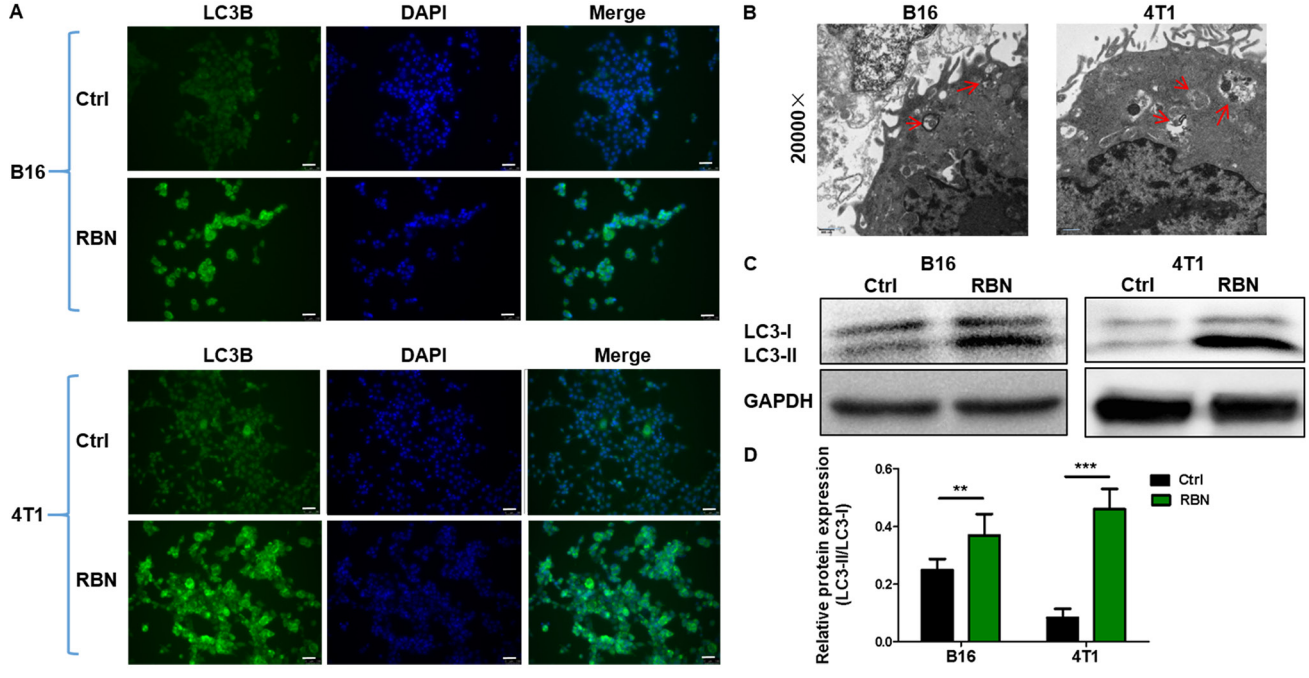

Figure 1. Generation of DRibbles by treatment with an autophagy inducer, a proteasome inhibitor, and a lysosomal inhibitor. (A, B) B16F10 and 4T1 cells were incubated with rapamycin (25 nM), bortezomib (100 nM), and NH_4Cl (10 mM) for 8–12 h. A) Immunofluorescence detection of the autophagy marker LC3B in B16F10 (upper panel) and 4T1 (lower panel) cells (scale bars: 25 μm). B) Detection of autophagosomes/autolysosomes in B16F10 (left panel) and 4T1 (right panel) cells by transmission electron microscopy (scale bars: 0.5 μm). C) B16F10 and 4T1 cells were incubated with rapamycin (25 nM), bortezomib (100 nM), and NH_4Cl (10 mM) for 24–48 h. Western blotting of the autophagy marker LC3-II/LC3-I in B16F10 (left panel) and 4T1 (right panel) cells. D) Statistical analysis of the western blotting results. Abbreviations: Ctrl-negative control; RBN-rapamycin+bortezomib+NH_4Cl; B16-B16F10. Bars and error bars represent means ± SD, respectively, of three independent experiments. **p<0.01, ***p<0.001 by Student's t-test

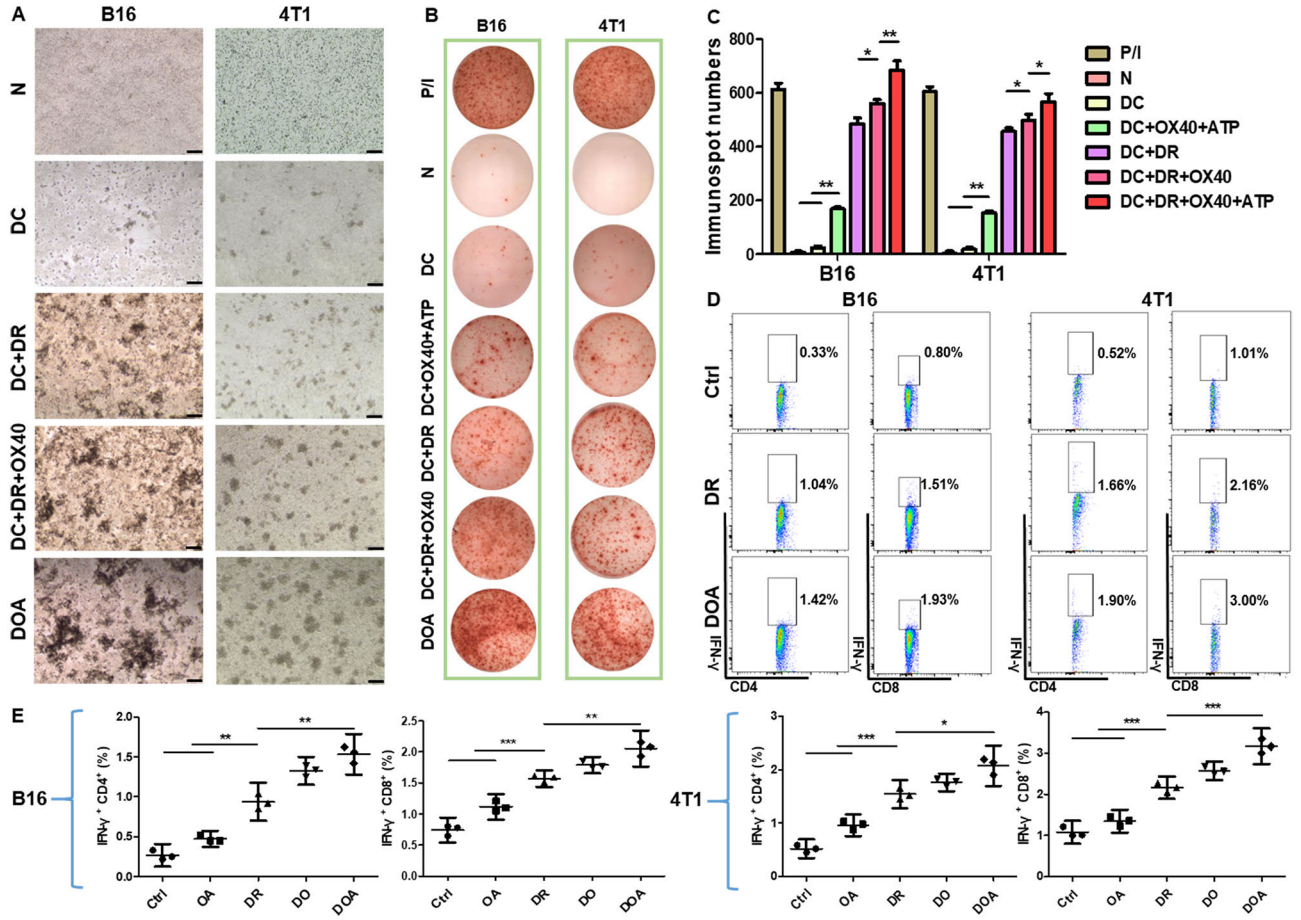

Figure 2. T cell activation *in vitro* by autophagosome-enriched DRibbles plus immune adjuvants. A) Splenic T cells were isolated from B16F10 tumor-bearing C57BL/6 mice (left panel) and 4T1 tumor-bearing BABL/c mice (right panel) locally treated with a Chemotherapy/Autophagy-Enhancing Regimen and incubated with vehicle or B16F10/4T1 derived DRibbles (20 μg/ml), and the immune adjuvants anti-OX40 antibody (10 μg/ml) and ATP (250 nM). Lymphocyte aggregates of mixed lymphocyte reactions (MLR) from various treatments (N, DC, DC+DR, DC+DR+OX40, DOA) were observed and imaged by light microscopy (scale bars: 50 μm). B) ELISpot analysis of immune responses to T cells in response to various treatments (P/I, N, DC, DC+OX40+ATP, DC+DR, DC+DR+OX40, DOA). C) Graphs of the ImmunoSpot numbers in B. D) Flow cytometric analysis of CD4/CD8 surface and intracellular cytokine (IFN-γ) expression to detect the activation of splenic T cells from B16F10 and 4T1 mice incubated with vehicle or DRibbles, anit-OX40 antibody and ATP. E) Graph of the results in D. Abbreviations: P/I-PMA+ionomycin (positive control); N-vehicle (negative control); DC-dendritic cells; DR-DRibbles; O-anti-OX40; DOA-DC+DR+OX40+ATP; **p<0.01, ***p<0.001 by Student's t-test

other combinations of reagents. These splenic T-cells were specifically extracted from B16F10 and 4T1 mice with tumors locally treated with a Chemotherapy/Autophagy-Enhancing Regimen [25]. Subtyping by flow cytometry showed that treatment with DRibbles, anti-OX40 antibody, and ATP activated larger numbers of functional CD4+ T cells and CD8+ T cells than did other reagent combinations (Figures 2D, 2E). These findings strongly demonstrated that B16F10/4T1-derived autophagosome-enriched DRibbles combined with anti-OX40 antibody and ATP could activate T-cells effectively *in vitro*.

Vaccination with B16F10/4T1-DRibbles and immune adjuvants strongly inhibited the growth of B16F10 cell-/4T1 cell-derived tumors *in vivo*. We next tested whether B16F10/4T1-derived autophagosome-enriched DRibbles combined with anti-OX40 antibody and ATP were effective *in vivo*. Melanomas were induced in C57BL/6 mice by injection of B16F10 cells, and breast carcinomas were induced in BALB/c mice by injecting 4T1 cells, followed by vaccination with various combinations of reagents (Figures 3A, 3E). Treatment with DRibbles plus anti-OX40 antibody showed greater inhibition of tumor growth than treatment with either reagent alone, with these two reagents plus ATP having the greatest antitumor activity for B16F10 cell-derived tumors (Figures 3B, 3C) and for 4T1 cell-derived tumors (Figures 3F, 3G). Treatment with DRibbles, anti-OX40 antibody, and ATP prolonged the survival of mice with both B16F10- (Figure 3D) and 4T1-derived (Figure 3H) tumors. Taken together, these data suggested that combinations of autologous DRibbles with anti-OX40 antibody and

ATP triggered systemic anti-tumor immune responses and effectively inhibited tumor growth in these *in vivo* models.

Induction of a systemic anti-tumor immune response by combination treatment. Immunological changes induced by treatment with DRibbles, anti-OX40 antibody, and ATP were assessed by IHC and flow cytometry analyses of the tumor, spleen, and peripheral blood. IHC showed that infiltration by CD3+, CD4+, and CD8+ T cells was significantly greater in B16F10-derived tumor tissues of mice administered the three reagents than in mice administered DRibbles alone or PBS (Figure 4A). T cells infiltration increased two- to four-fold: [DR+OX40+ATP vs. control: approximately 8% vs. 3% of CD3+, 4% vs. 1% of CD4+, and 5% vs. 2% of CD8+ T cells]. Meanwhile, FoxP3+ T cells (Tregs) significantly reduced: 42% vs. 24% of CD4+ T cells (Figure 4B). Similar results were observed in the 4T1 tumor model (Figures 4C, 4D).

Systemic immune responses were assessed by measuring the levels of IFN-γ-producing T cells in the spleen and peripheral blood of tumor-bearing mice by flow cytometry. Splenic CD4+ T cells and CD8+ T cells from B16F10 mice vaccinated with DR, OX40, and ATP secreted greater amounts of IFN-γ than mice vaccinated with PBS, OX40, DR, or DR+OX40

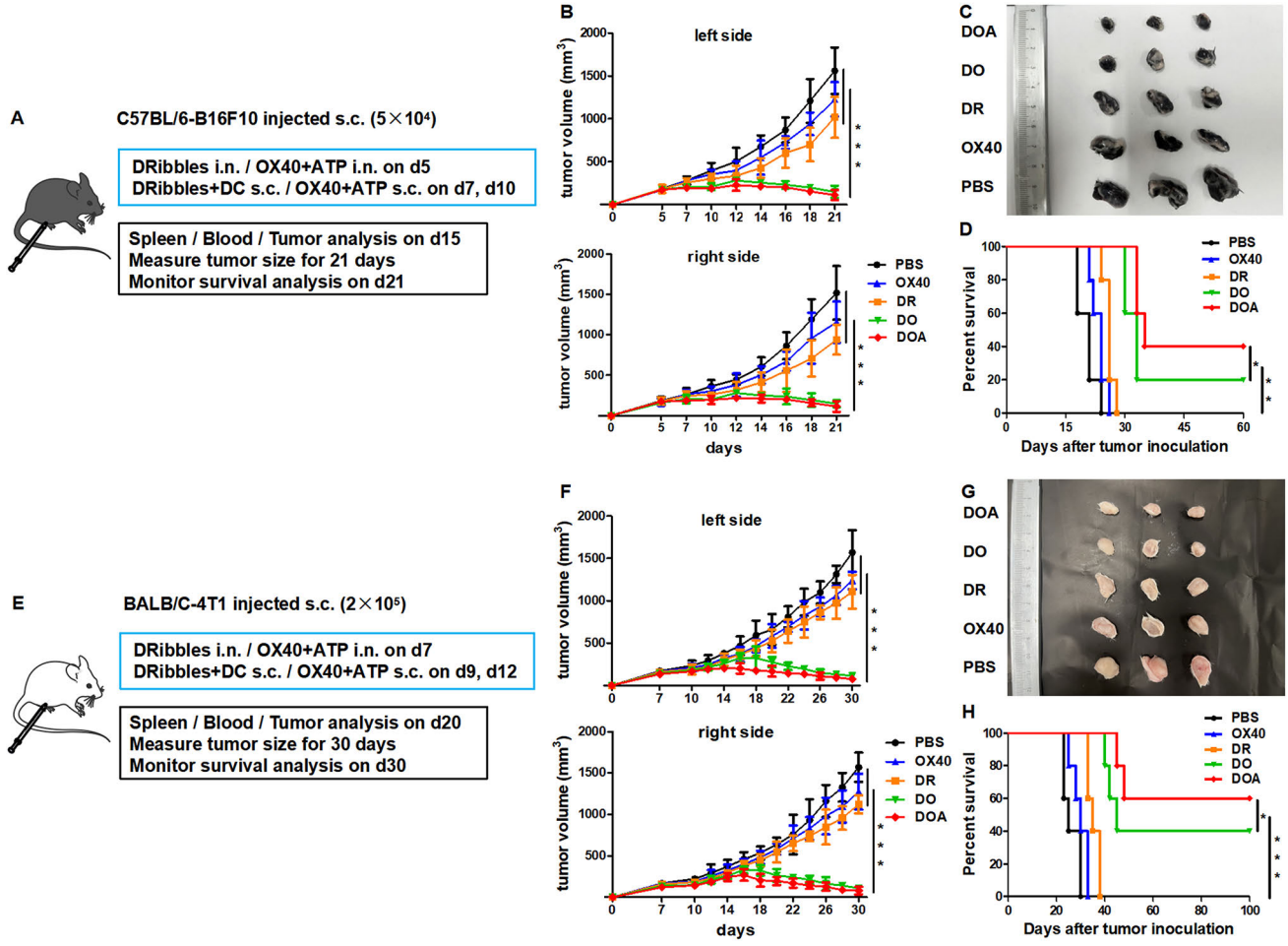

Figure 3. Inhibition of *in vivo* tumor growth by vaccination with DRibbles, anti-OX40, and ATP. A) Treatment scheme of B16F10 cell-derived tumors. B16F10 cells (5×10⁴) were subcutaneously (s.c.) injected into each of the bilateral abdominal fat pads of C57BL/6 mice. On day 5, mice were administered DRibble vaccines (20 μg) with or without anti-OX40 antibody (60 μg) and ATP (200 μg), followed by two boosts with DRibble-loaded DCs (20 μg/3 million, s.c.), with or without anti-OX40 (60 μg) and ATP (200 μg), on days 7 and 10. B) Individual growth curves of bilateral tumors in C57BL/6 mice bearing B16F10 tumors treated with vehicle or DRibbles and immune adjuvants. C) Representative images of B16F10 cell-derived tumors on day 15. D) Survival curves of C57BL/6 mice bearing B16F10 cell-derived tumors. E) Treatment scheme of 4T1 cell-derived tumors. 4T1 cells (2×10⁵) were injected s.c. into each of the bilateral mammary fat pads of BALB/c mice. On day 7, mice were administered DRibble vaccines (20 μg), with or without anti-OX40 (60 μg) and ATP (200 μg), followed by two boosts with DRibble-loaded DCs (20 μg/3 million, s.c.), with or without anti-OX40 (60 μg) and ATP (200 μg), on days 9 and 12. F) Individual growth curves of bilateral tumors in BALB/c mice bearing 4T1 tumors treated with vehicle or DRibbles and immune adjuvants. G) Representative images of 4T1 cell-derived tumors on day 20. H) Survival curves of C57BL/6 mice bearing B16F10 cell-derived tumors. n=5–6 mice/group. Phosphate-buffered saline (PBS) was used as a control. Abbreviations: DR-DRibbles; DO-DR+OX40; DOA-DR+OX40+ATP; *p<0.05, **p<0.01, ***p<0.001 by Student's t-test

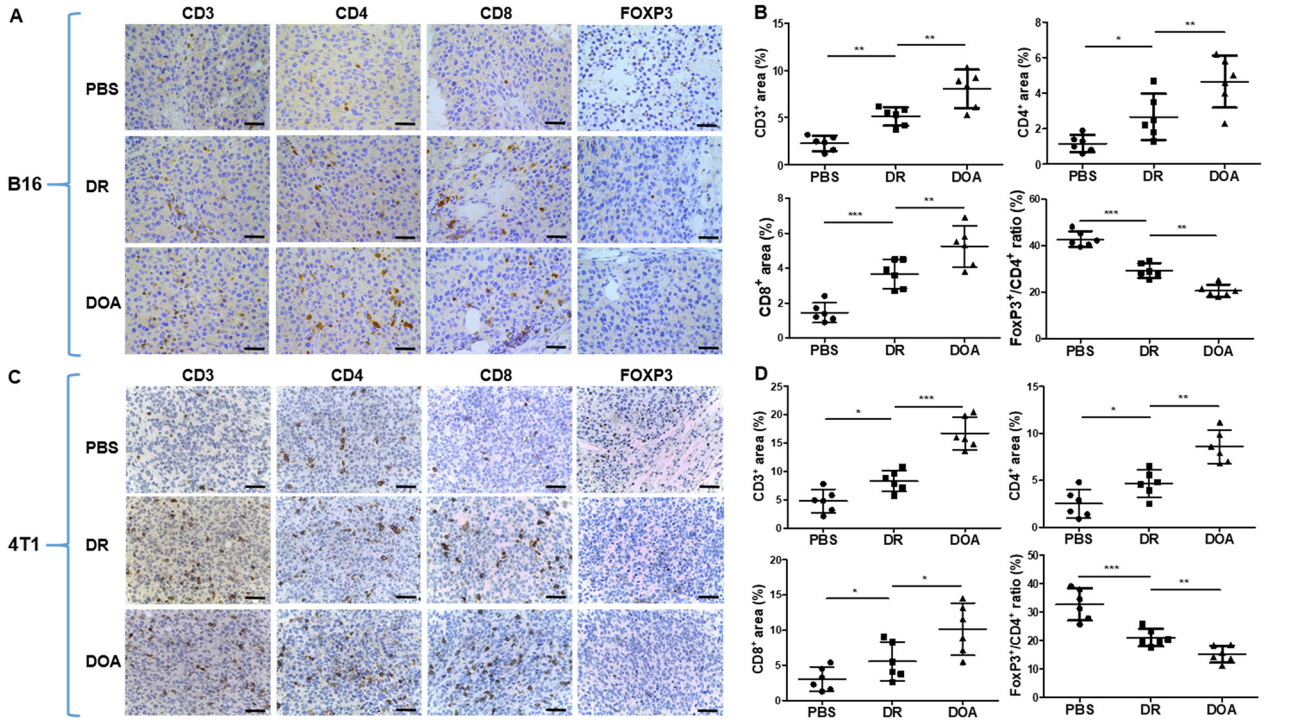

Figure 4. Immunological analysis of the local and systemic effects of treatment with DRibbles, anti-OX40 antibody, and ATP. A, C) Immunological analysis of B16F10 (A) and 4T1 (C) mouse tumors after treatment. Representative images showing immunohistochemical (IHC) staining of CD3, CD4, CD8, and FOXP3 in B16F10 tumor samples on day 15 and in 4T1 tumor samples on day 20 (scale bars: 50 μm). B, D) Graphs of the IHC staining results of B16F10 (B) and 4T1 (D) tumors. Abbreviations: DR-DRibbles; DO-DR+OX40; DOA-DR+OX40+ATP; *p<0.05, **p<0.01, ***p<0.001 by Student's t-test

(Figure 5A). Treatment with DR, OX40, and ATP resulted in a greater increase in CD8+ T cells (2.32%) than in CD4+ T cells (1.64%) but reduced the numbers of Tregs (3.20%) in the spleen (Figure 5B). Analysis of blood samples showed increases in CD8+ T cells (2.27%) and CD4+ T cells (1.99%) but reductions in Tregs (4.21%) (Figures 5C, 5D). Similar results were obtained in mice bearing 4T1-derived tumors (Figures 5E–5H; Supplementary Figures S1A, S1B).

Incubation of splenic T cells with B16/4T1-DRibbles or B16/4T1 cell lysates. To further clarify the mechanisms by which vaccination with DRibbles, anti-OX40 antibody, and ATP triggered systemic antitumor immunity in two cancer models, cells were stimulated *ex vivo* to determine whether specific T cells targeting tumor or DRibbles-derived antigens were generated, as well as to compare the antigenic activities of tumor antigens and DRibbles. Splenocytes from B16F10-bearing C57BL/6 mice and 4T1-bearing BALB/c mice treated with DRibbles, anti-OX40 antibody, and ATP were stimulated with mature DCs loaded with B16/4T1-DRibbles or B16F10/4T1 cell lysates. IFN-γ ELISpot assays showed that splenocytes from mice treated with the three reagents exhibited a stronger response to B16/4T1-DRibbles and B16/4T1 cell-derived antigens than did splenocytes from control mice. In addition, DRibbles had greater antigenic activity than tumor cell lysates (Figures 6A, 6B).

The responses of T cells in the different groups were further analyzed by flow cytometry to determine the levels of the intracellular cytokines IFN-γ and TNF-α. Cells from mice vaccinated with DRibbles, anti-OX40 antibody, and ATP showed higher levels of intracellular cytokines than cells from the other groups. The incubation of DRibbles or tumor lysates with splenic T cells derived from B16F10-bearing or 4T1-bearing mice vaccinated with DRibbles and anti-OX40 antibody and ATP led to the activation of a greater number of tumor antigen-specific CD8+ T cells (Figures 6C–6F) and CD4+ T cells (Figures 7A–7D) than did incubation with splenic T cells derived from the other groups of mice (Supplementary Figures S2A–S2D). In addition, B16/4T1-DRibbles, as a source of tumor antigens, were better activators of antigen-specific CD8+ and CD4+ T cells than B16/4T1 cell lysates. These results showed that, compared with other treatments, the combination of DRibbles and anti-OX40 antibody and ATP induced greater numbers of antigen-specific T cells *in vivo* and that DRibbles showed greater antigenic activity than tumor cell lysates.

B16/4T1-DRibbles combination vaccines induce neoantigen-specific T-cell responses. Autophagosome-enriched DRibbles were shown to preserve many tumor antigens, including long-lived and short-lived proteins and incomplete ribosome products. Moreover, DRibble cancer vaccines

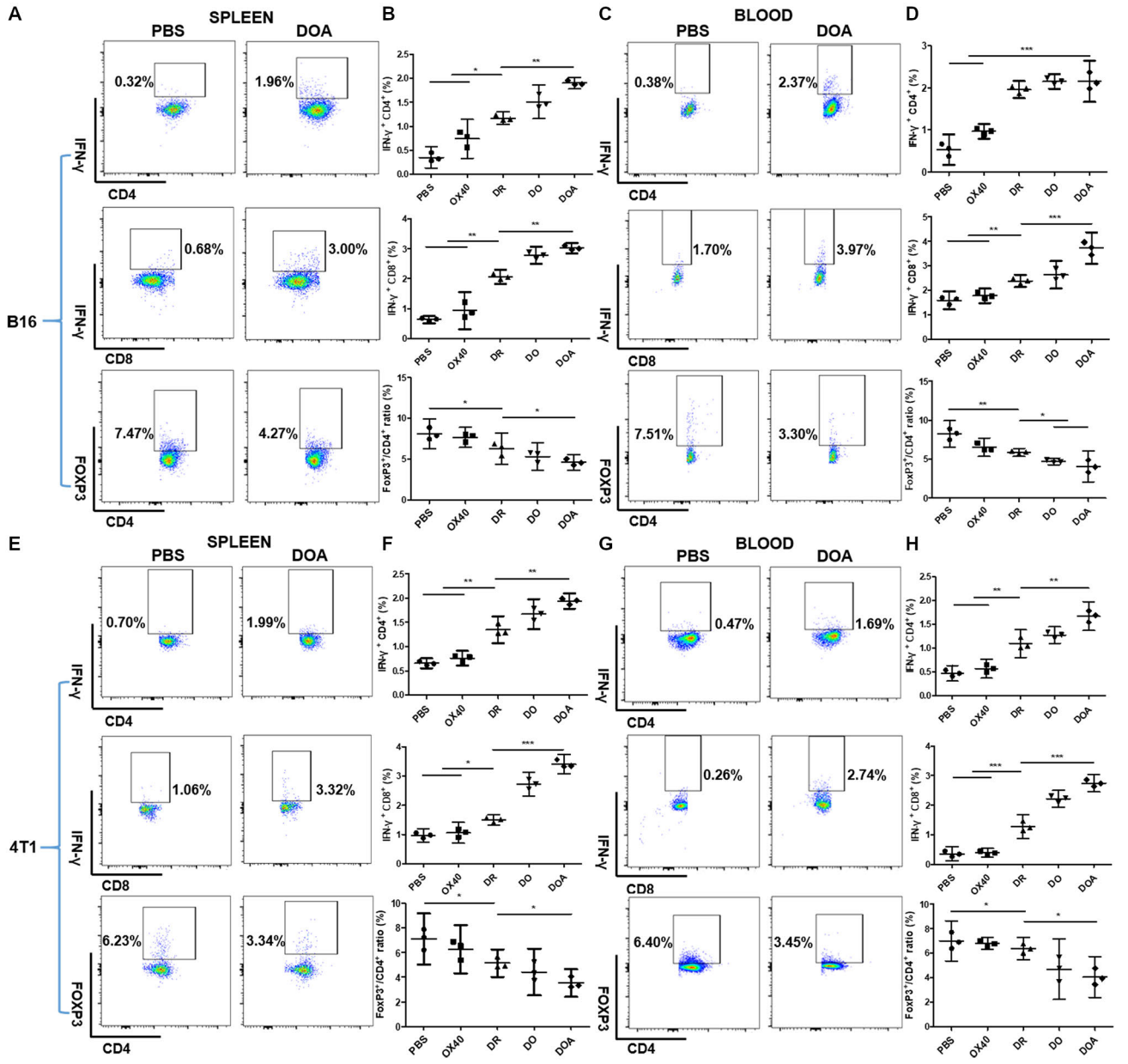

Figure 5. Immunological analysis of the local and systemic effects of treatment with DRibbles, anti-OX40 antibody, and ATP. A, C) Flow cytometry analysis of the percentages of IFN-γ-producing CD4+ T cells, CD8+ T cells, and FoxP3+ T cells on day 15 in the spleen (A) and peripheral blood (C) samples from mice with B16F10 tumors treated with PBS, OX40, DR, DO, and DOA. B, D) Graphs of the flow cytometry results of spleen (B) and peripheral blood (D) samples in mice with B16F10 tumors. E, G) Flow cytometry analysis of the percentages of IFN-γ-producing CD4+ T cells, CD8+ T cells, and FoxP3+ T cells on day 20 in the spleen (E) and peripheral blood (G) samples from mice with 4T1 tumors treated with PBS, OX40, DR, DO, and DOA. F, H) Graphs of the flow cytometry of spleen (F) and peripheral blood (H) samples from mice with 4T1 tumors. Abbreviations: DR-DRibbles; DO-DR+OX40; DOA-DR+OX40+ATP; *p<0.05, **p<0.01, ***p<0.001 by Student's t-test

were able to target hidden tumor antigen epitopes [12, 14]. Although DRibbles contain shared tumor-associated antigens, it is unclear whether DRibbles contain tumor-specific neoantigens that are key targets for antitumor immune responses. We, therefore, evaluated whether DRibbles contained neoantigens, a finding that would be expected if vaccination with B16/4T1-DRibbles plus anti-OX40 antibody and ATP efficiently activated the immune response of neoantigen-specific T-cells. Responsive mutant neoantigen peptides from B16F10 and 4T1 cells were therefore synthesized and prescreened [25, 26] (Supplementary Figures S3A, S3B). Two optimal mutant peptides (B16-M27 and B16-M30) derived from B16F10 cells and two (4T1-M8 and 4T1-M17) from 4T1 cells were used for the subsequent experiments. Spleno-

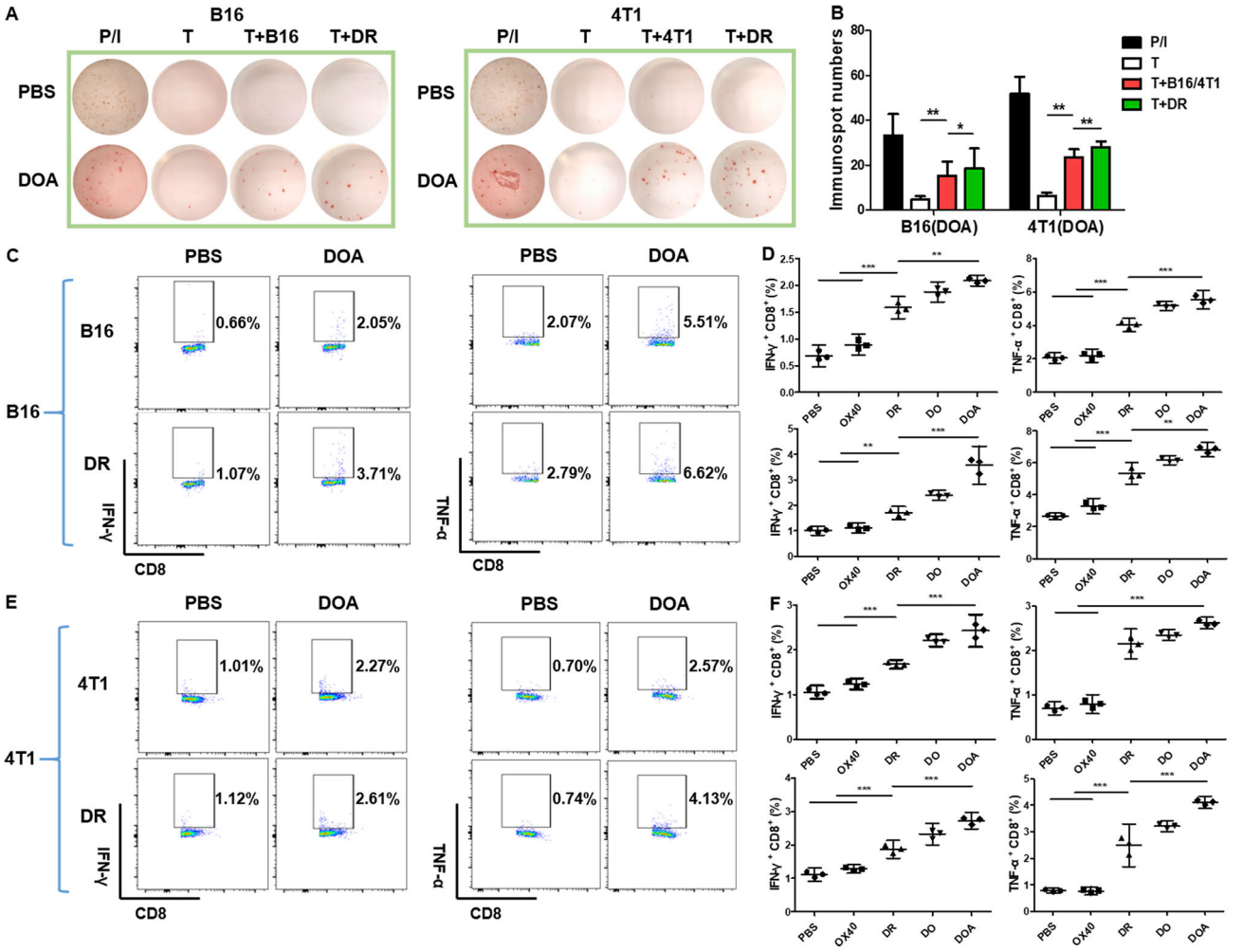

Figure 6. Antigenic activities of T cells extracted from mice administered DOA reacted with B16/4T1-DRibbles and B16/4T1 cell lysates. A) IFN-γ ELISpot assays of immune responses of splenic T cells isolated from B16F10 tumor-bearing C57BL/6 mice and 4T1 tumor-bearing BALB/c mice treated with PBS, OX40, DR, DO, and DOA and incubated with B16/4T1-DRibbles or B16/4T1 cell lysates. B) Graph of the results in A. C, E) Flow cytometry analysis of CD8 surface and intracellular cytokine (IFN-γ and TNF-α) expression to detect the activation of splenic T cells incubated with B16/4T1-DRibbles and B16F10/4T1 cell lysates. D, F) Graphs of the flow cytometry results of CD8+ T cells in the B16F10 (D) and 4T1 (F) tumor models. Abbreviations: DR-DRibbles; DO-DR+OX40; DOA-DR+OX40+ATP; *p<0.05, **p<0.01, ***p<0.001 by Student's t-test

cytes from C57BL/6 mice bearing B16F10 cell-derived tumors and vaccinated with DRibbles, anti-OX40 antibody, and ATP were incubated with DCs loaded with the peptide B16-M27 or B16-M30 to evaluate the neoantigen-reactive T cell immune response. IFN-γ ELISpot analysis showed that all the mutant peptide-loaded DCs activated T cells to secrete IFN-γ (Figures 8A, 8B). The composition of the neoantigen-reactive T-cell populations was determined by flow cytometry and the intracellular cytokines IFN-γ and TNF-α were analyzed. When incubated with neoantigen peptides, splenic T cells isolated from C57BL/6 mice bearing B16F10 cell-derived tumors and vaccinated with DRibbles and anti-OX40 antibody and ATP generated more activated CD4+ and CD8+ T cells than cells isolated from mice in the other treatment groups (Figures 8C–8F). Specifically, B16-M30 treatment increased IFN-γ and TNF-α levels by 1.41% and 1.84%, respectively, in CD8+ T cells and by 1.36% and 2.01%, respectively, in CD4+ T cells. In addition, B16-M27 treatment increased these levels by 1.35% and 1.57%, in CD8+ T cells and by 1.26% and 2.07%, respectively, in CD4+ T cells.

Similar results were obtained from BALB/c mice bearing 4T1 cell-derived tumors, further confirming that vaccination with DRibbles and anti-OX40 antibody and ATP could enhance neoantigen-specific T cell responses. Specifically, 4T1-M8 treatment increased IFN-γ and TNF-α levels by 3.13% and 4.26%, respectively, in CD8+ T cells and by 2.11% and 2.38%, respectively, in CD4+ T cells; whereas 4T1-M17 increased these levels by 2.74% and 3.05%, respectively,

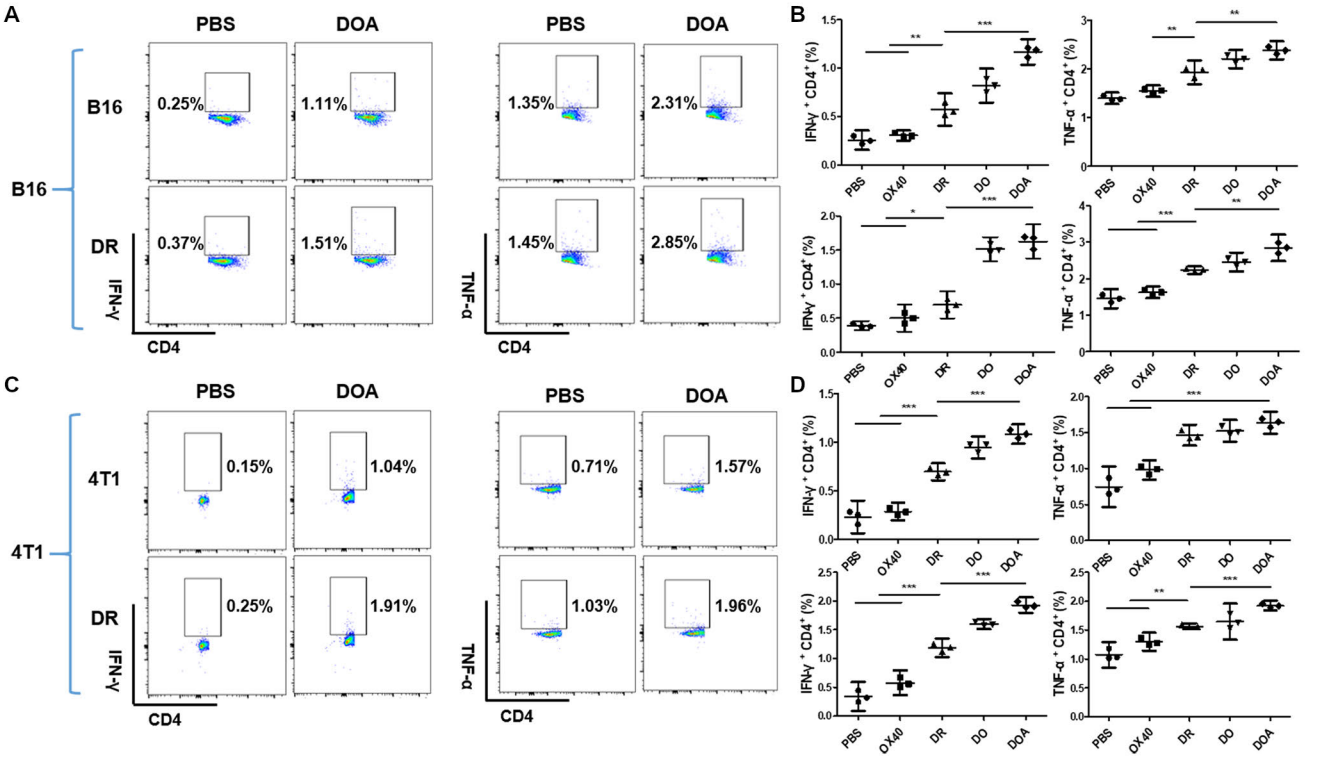

Figure 7. Antigenic activities of T cells extracted from mice administered DOA reacted with B16/4T1-DRibbles and B16/4T1 cell lysates. A, C) Flow cytometry analysis of CD4 surface and intracellular cytokine (IFN-γ and TNF-α) expression to detect the activation of splenic T cells incubated with B16/4T1-DRibbles and B16F10/4T1 cell lysates. B, D) Graph of the flow cytometry results of CD4+ T cells in the B16F10 (B) and 4T1 (D) tumor models. Abbreviations: DR-DRibbles; DO-DR+OX40; DOA-DR+OX40+ATP; *p<0.05, **p<0.01, ***p<0.001 by Student's t-test

in CD8+ T cells and by 2.00% and 2.06%, respectively, in CD4+ T cells (Figures 8G–8L). These findings indicate that the antitumor efficacy of DRibbles combination vaccines is largely due to the activation of neoantigen-specific T cells (Supplementary Figures S4A–S4D).

Autophagosome formation has been shown to positively correlate with the expression of the regulatory genes ATG8 and ATG12 [27]. Analysis of the relationship between ATG8/12 and immune cell infiltration levels in human breast carcinoma (BRCA) and skin cutaneous melanoma (SKCM) in a bioinformatics database showed that the expression of ATG8 and ATG12 was positively correlated with the infiltration of CD8+ T cells (maximum correlation), CD4+ T cells, and DCs in BRCA and SKCM tissues (Supplementary Figures S3C, S3D). Taken together, these findings indicate that tumor-derived autophagosome vaccines combined with immune adjuvants can promote the activation of neoantigen-specific T-cells, thus mediating the antitumor immune response (Figure 9).

Discussion

Cancer vaccines based on peptides, tumor-associated antigens, and whole tumor cells have been used in immunotherapy trials of patients with melanoma, breast, and colorectal cancer. Although the efficacy of these therapeutic cancer vaccines has increased, overall clinical outcomes remain unsatisfactory mainly because of tumor immune escape, immunosuppressive microenvironments, and low immunogenicity [28–30]. The findings in the present study may contribute to the development of methods to effectively enhance the release and presentation of multiple tumor antigens, especially neoantigens, improving immunogenicity-mediated anti-tumor immune responses and reversing immune suppression.

The T cell co-stimulatory molecule OX40 and its cognate ligand OX40L are important therapeutic targets for tumor immunotherapy. Anti-OX40 co-stimulatory antibody could directly influence the expansion of effector T cells and the inhibition of Tregs. Clinically, this antibody was found to be well-tolerated and to have some anti-tumor activity [31–34]. In addition, the combination of DRibbles and anti-OX40 antibody was found to induce cross-reactive T-cell immune responses and tumor regression in mouse tumor models [13].

An endogenous adjuvant is the body's own, and the use of an endogenous adjuvant is safer and has fewer side effects. Endogenous substances as new vaccine adjuvants have attracted more and more attention. ATP is a common

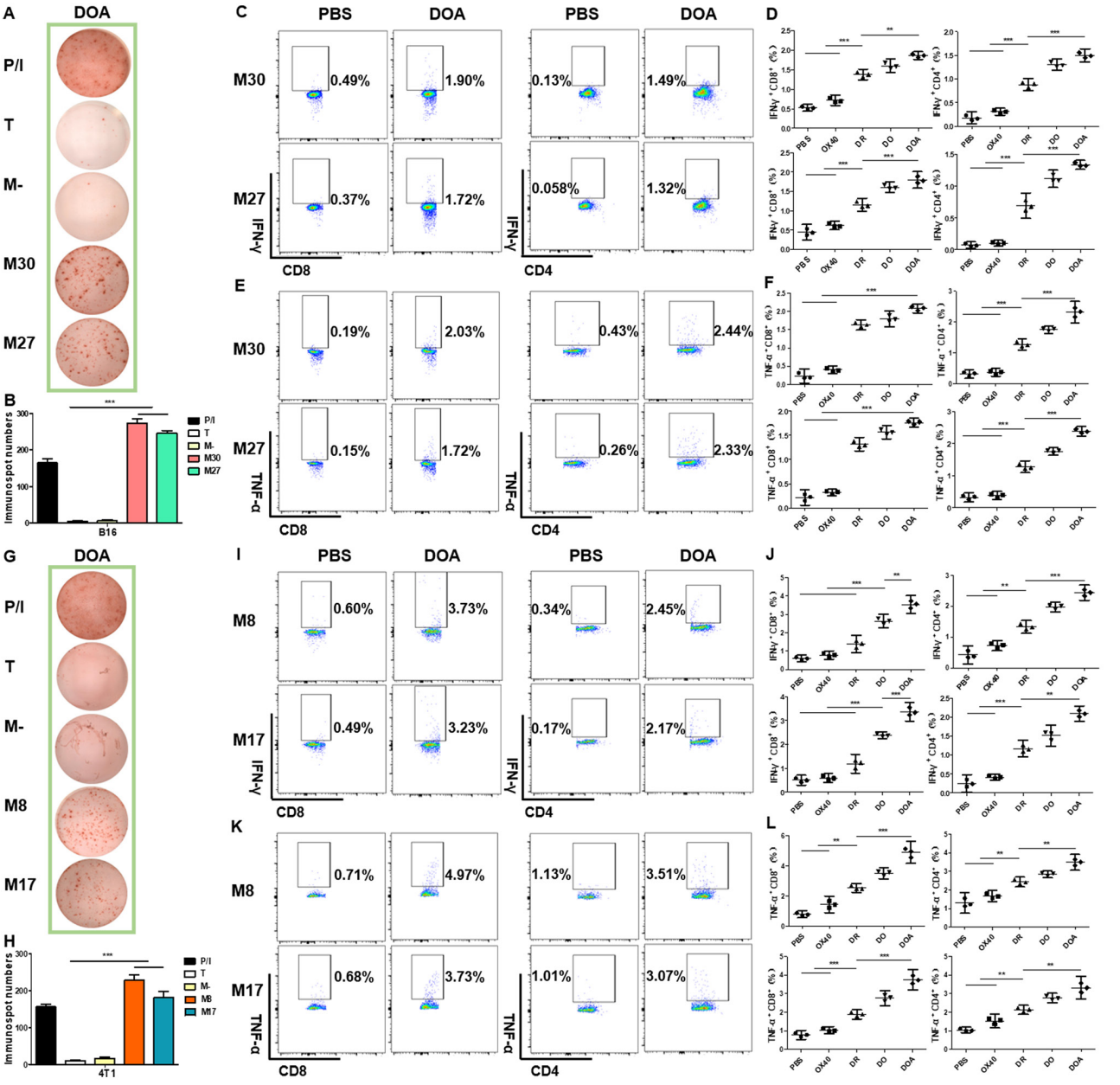

Figure 8. Induction of neoantigen-specific T-cell responses by vaccination with DRibbles, anti-OX40 antibody, and ATP. A) IFN-γ ELISpot analysis of immune responses of splenic T cells targeting neoantigens from B16F10 cell-derived, tumor-bearing C57BL/6 mice treated with PBS, OX40, DR, DO, and DOA following stimulation with mature BMDCs plus the neoantigen peptides M30 and M27. B) Graph of the results in A for the B16F10 model. C, E) Flow cytometry analysis of the expression of the intracellular cytokines IFN-γ (C) and TNF-α (E) during neoantigen-specific T cell immune responses in the B16F10 model. D, F) Graphs of the flow cytometry results of IFN-γ (D) and TNF-α (F) expression in the B16F10 mouse model. G) IFN-γ ELISpot analysis of immune responses of splenic T cells targeting neoantigens from 4T1 cell-derived, tumor-bearing BABL/c mice treated with PBS, OX40, DR, DO, and DOA following stimulation with mature BMDCs plus the neoantigen peptides M8 and M17. H) Graph of the results in G for the 4T1 model. I, K) Flow cytometry analysis of the expression of the intracellular cytokines IFN-γ (I) and TNF-α (K) during neoantigen-specific T cell immune responses in the 4T1 model. J, L) Graphs of the flow cytometry of IFN-γ (J) and TNF-α (L) expression in the 4T1 mouse model. Abbreviations: N-no peptide; M- -negative peptide; DR-DRibbles; DO-DR+OX40; DOA-DR+OX40+ATP; *p<0.05, **p<0.01, ***p<0.001 by Student's t-test

intracellular metabolite required for cell viability. ATP can also act as an effective immune adjuvant to enhance specific anti-tumor immune response [17, 18]. ATP secreted by dying tumor cells acts as an important "find-me" signal for antigen-presenting cells, as well as stimulating the tumor infiltration of cytotoxic T lymphocytes. ATP binds to the P2X and P2Y purine receptors on DCs to activate NALP3-ASC-inflammasomes, which leads to the release of the immuno-

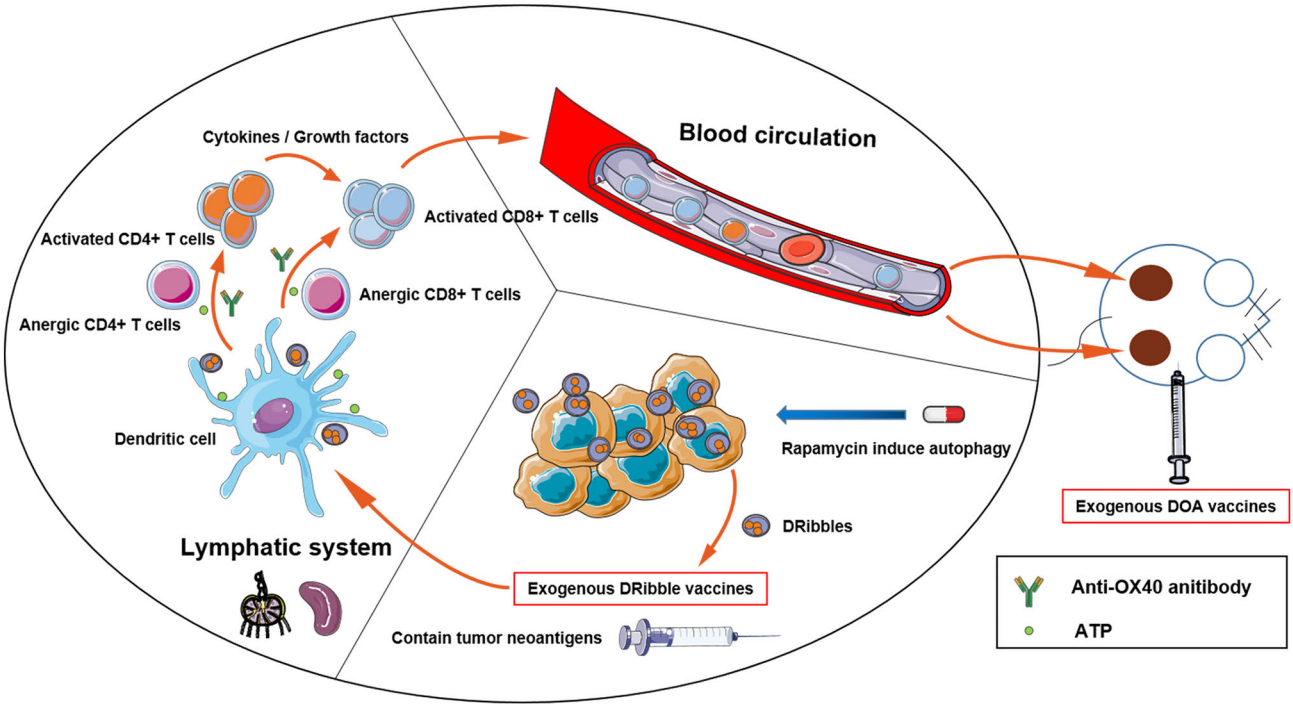

Figure 9. Schematic diagram summarizing the findings of this study. Exogenous DRibble vaccines combined with anti-OX40 antibody and ATP induced neoantigen-specific T-cell responses.

modulator IL-1β. IL-1β promotes the activation of IFN-γ secreting T-cells. ATP is also involved in DC maturation and homing [15, 16]. The combination of anti-OX40 antibody and ATP might therefore synergistically enhance the anti-tumor immune responses induced by cancer vaccines. In the early stage, we had verified that T cell aggregation could be recruited by inducing cell death in situ by chemotherapy drugs, and related research also showed that chemotherapy drugs could make tumor cells release ATP to recruit immune cells [25]. On this basis, we added a certain dose of ATP and found that the aggregation of T cells increased under the microscope and the activity of T-cells increased to some extent *in vitro*. Furthermore, it could induce potent systemic anti-tumor immune responses and mediate significant tumor regression in C57BL/6 mice bearing B16F10 tumors models and in BALB/c mice bearing 4T1 tumors.

More powerful T-cell immune responses could be induced if hidden antigenic epitopes, especially neoantigen epitopes, could be exposed and delivered to antigen-presenting cells (APCs) for efficient presentations [35, 36]. Tumor-derived autophagosome-based therapeutic DRibble vaccine was shown to effectively induce tumor-reactive CD8+ T cells via cross-presentation [22–24]. DRibble vaccines, which contain both heat shock proteins (HSPs) and ubiquitinated short-lived proteins (SLiPs), were found to play an important role in preserving the antigen repertoire and enhancing anti-tumor responses. HSPs and SLiPs, however, contain two different pools of antigens. HSPs purified from tumor cells are thought to contain tumor-specific antigens and thus would be expected to provide special protection for the same type of tumor. In contrast, SLiPs provide shared antigens and can induce cross-protection against challenge with different types of tumors. These findings suggest that because of their doubly protective activity (i.e., specific and cross-protection), DRibble vaccines would be ideal partners for co-stimulatory antibodies, immune checkpoint blockade (ICB), and other immune adjuvants. Correlation studies extend their observations to mammary carcinomas from mice of different genetic backgrounds. They demonstrated that combined intranodal administration of autologous or allogeneic DRibbles together with anti-OX40 antibody led to robust proliferation, expansion, and differentiation of memory and effector T-cells. DRibble cancer vaccines have the potential ability to target hidden tumor antigen epitopes, including both neoantigens and shared tumor-associated antigens, thus enhancing the immune responses of antigen-specific T-cells [11–14].

Although DRibbles contain shared tumor-associated epitopes that could induce cross-reactive T-cell immune responses and tumor regression, it is unclear whether DRibbles contribute to the exposure of specific neoantigen epitopes. We showed that splenocytes from mice vaccinated with DRibbles and immune adjuvants could activate more neoantigen-specific CD4+ T and CD8+ T cells, indicating

that DRibbles contain neoantigens and can enhance tumor immunogenicity. In addition, B16/4T1-DRibbles, as a source of tumor antigens, were better activators of antigen-specific T cells than proteins in B16/4T1 cell lysate, providing further indications that vaccination with DRibbles, anti-OX40 antibody, and ATP resulted in greater numbers of antigen-specific T cells. Finally, analyses of databases of patients with BRCA and SKCM revealed that the expression of the regulatory genes ATG8/12, a marker of autophagosome formation, was positively correlated with the infiltration of CD8+ T cells. On this basis, we need to further supplement the relevant findings about the effectiveness of heterologous DRibble vaccines to make the study more exciting.

In summary, this study showed that exogenous autophagosome-enriched DRibble vaccines combined with the immune adjuvants anti-OX40 antibody and ATP exhibit optimal immune stimulation and anti-tumor efficiency *in vitro* and *in vivo*. Tumor-derived autophagosome vaccines that contain specific neoantigens can enhance tumor immunogenicity, thus increasing the efficacy of anti-tumor treatment. Studies are needed, however, to determine the exact mechanism of action of these vaccines in these and other tumor models with high mutation rates. In addition, clinical trials are needed to assess the efficacy of vaccination with DRibbles and immune. The findings of the present study indicate, however, that DRibble vaccines could be valuable in cancer immunotherapy.

Supplementary information is available in the online version of the paper.

Acknowledgments: This study was supported by the National Key Research & Development Project (2016YFC1303404) of the Ministry of Science and Technology of the People's Republic of China, and the Chinese Society of Clinical Oncology-Hutchison Whampoa Medical Cancer Research Fund Project (Y-HH202101-0301). The authors are grateful to all the participants of the study as well as to Liangping Li, Xinyue Liang, Kecheng Liu, and Shili Chen.

References

[1] REBECCA LS, KIMBERLY DM, NIKITA SW, AHMEDIN J. Cancer statistics, 2023. CA Cancer J Clin 2023; 73: 17–48. https://doi.org/10.3322/caac.21763

[2] COUZIN-FRANKEL J. Breakthrough of the year 2013. Cancer immunotherapy. Science 2013; 342: 1432–1433. https://doi.org/10.1126/science.342.6165.1432

[3] LIANG J, ZHAO X. Nanomaterial-based delivery vehicles for therapeutic cancer vaccine development. Cancer Biol Med 2021; 18: 352–371. https://doi.org/10.20892/j.issn.2095-3941.2021.0004

[4] SAUNG MT, KE X, HOWARD GP, ZHENG L, MAO HQ. Particulate carrier systems as adjuvants for cancer vaccines. Biomater Sci 2019; 7: 4873–4887. https://doi.org/10.1039/c9bm00871c

[5] WILSON JT. A sweeter approach to vaccine design. Science 2019; 363: 584–585. https://doi.org/10.1126/science.aav9000

[6] BLASS E, OTT PA. Advances in the development of personalized neoantigen-based therapeutic cancer vaccines. Nat Rev Clin Oncol 2021; 18: 215–229. https://doi.org/10.1038/s41571-020-00460-2

[7] MOUGEL A, TERME M, TANCHOT C. Therapeutic Cancer Vaccine and Combinations With Antiangiogenic Therapies and Immune Checkpoint Blockade. Front Immunol 2019; 10: 467. https://doi.org/10.3389/fimmu.2019.00467

[8] YU L, CHEN Y, TOOZE SA. Autophagy pathway: Cellular and molecular mechanisms. Autophagy 2018; 14: 207–215. https://doi.org/10.1080/15548627.2017.1378838

[9] DIKIC I, ELAZAR Z. Mechanism and medical implications of mammalian autophagy. Nat Rev Mol Cell Biol 2018; 19: 349–364. https://doi.org/10.1038/s41580-018-0003-4

[10] HUSSEY S, TRAVASSOS LH, JONES NL. Autophagy as an emerging dimension to adaptive and innate immunity. Semin Immunol 2009; 21: 233–241. https://doi.org/10.1016/j.smim.2009.05.004

[11] SU H, LUO Q, XIE H, HUANG X, NI Y et al. Therapeutic antitumor efficacy of tumor-derived autophagosome (DRibble) vaccine on head and neck cancer. Int J Nanomedicine 2015; 10: 1921–1930. https://doi.org/10.2147/IJN.S74204

[12] LI Y, WANG LX, PANG P, CUI Z, AUNG S et al. Tumor-derived autophagosome vaccine: mechanism of cross-presentation and therapeutic efficacy. Clin Cancer Res 2011; 17: 7047–7057. https://doi.org/10.1158/1078-0432.CCR-11-0951

[13] YU G, LI Y, CUI Z, MORRIS NP, WEINBERG AD et al. Combinational Immunotherapy with Allo-DRibble Vaccines and Anti-OX40 Co-Stimulation Leads to Generation of Cross-Reactive Effector T Cells and Tumor Regression. Sci Rep 2016; 6: 37558. https://doi.org/10.1038/srep37558

[14] LI Y, WANG LX, YANG G, HAO F, URBA WJ et al. Efficient cross-presentation depends on autophagy in tumor cells. Cancer Res 2008; 68: 6889–6895. https://doi.org/10.1158/0008-5472.CAN-08-0161

[15] SUN L, SHEN F, TIAN L, TAO H, XIONG Z et al. ATP-Responsive Smart Hydrogel Releasing Immune Adjuvant Synchronized with Repeated Chemotherapy or Radiotherapy to Boost Antitumor Immunity. Adv Mater 2021; 33: e2007910. https://doi.org/10.1002/adma.202007910

[16] WANG X, LI M, REN K, XIA C, LI J et al. On-Demand Autophagy Cascade Amplification Nanoparticles Precisely Enhanced Oxaliplatin-Induced Cancer Immunotherapy. Adv Mater 2020; 32: e2002160. https://doi.org/10.1002/adma.202002160

[17] FADER CM, AGUILERA MO, COLOMBO MI. ATP is released from autophagic vesicles to the extracellular space in a VAMP7-dependent manner. Autophagy 2012; 8: 1741–1756. https://doi.org/10.4161/auto.21858

[18] MARTIN S, DUDEK-PERIC AM, GARG AD, ROOSE H, DEMIRSOY S et al. An autophagy-driven pathway of ATP secretion supports the aggressive phenotype of BRAFV600E inhibitor-resistant metastatic melanoma cells. Autophagy 2017; 13: 1512–1527. https://doi.org/10.1080/15548627.2017.1332550

[19] LANCASTER EM, JABLONS D, KRATZ JR. Applications of Next-Generation Sequencing in Neoantigen Prediction and Cancer Vaccine Development. Genet Test Mol Biomarkers 2020; 24: 59–66. https://doi.org/10.1089/gtmb.2018.0211
[20] HAN XJ, MA XL, YANG L, WEI YQ, PENG Y et al. Progress in Neoantigen Targeted Cancer Immunotherapies. Front Cell Dev Biol 2020; 8: 728. https://doi.org/10.3389/fcell
[21] JIANG T, SHI T, ZHANG H, HU J, SONG Y et al. Tumor neoantigens: from basic research to clinical applications. J Hematol Oncol 2019; 12: 93. https://doi.org/10.1186/s13045-019-0787-5
[22] DONG H, SU H, CHEN L, LIU K, HU HM et al. Immunocompetence and mechanism of the DRibble-DCs vaccine for oral squamous cell carcinoma. Cancer Manag Res 2018; 10: 493–501. https://doi.org/10.2147/CMAR.S155914
[23] SANBORN RE, ROSS HJ, AUNG S, ACHESON A, MOUDGIL T et al. A pilot study of an autologous tumor-derived autophagosome vaccine with docetaxel in patients with stage IV non-small cell lung cancer. J Immunother Cancer 2017; 5: 103. https://doi.org/10.1186/s40425-017-0306-6
[24] YI Y, HAN J, ZHAO L, WANG C, FANG Y et al. Immune responses of dendritic cells combined with tumor-derived autophagosome vaccine on hepatocellular carcinoma. Chin J Cancer Res 2015; 27: 597–603. https://doi.org/10.3978/j.issn.1000-9604.2015.12.07
[25] YUAN J, YUAN X, WU K, GAO J, LI L. A Local and Low-Dose Chemotherapy/Autophagy-Enhancing Regimen Treatment Markedly Inhibited the Growth of Established Solid Tumors Through a Systemic Antitumor Immune Response. Front Oncol 2021; 11: 658254. https://doi.org/10.3389/fonc.2021.658254
[26] KREITER S, VORMEHR M, VAN DE RN, DIKEN M, LOWER M et al. Mutant MHC class II epitopes drive therapeutic immune responses to cancer. Nature 2015; 520: 692–696. https://doi.org/10.1038/nature14426
[27] NODA NN, FUJIOKA Y, HANADA T, OHSUMI Y, INAGAKI F. Structure of the Atg12-Atg5 conjugate reveals a platform for stimulating Atg8-PE conjugation. EMBO Rep 2013; 14: 206–211. https://doi.org/10.1038/embor.2012.208
[28] SAXENA M, VAN DER BSH, MELIEF CJM, BHARDWAJ N. Therapeutic cancer vaccines. Nat Rev Cancer 2021; 21: 360–378. https://doi.org/10.1038/s41568-021-00346-0
[29] SHAE D, BALJON JJ, WEHBE M, BECKER KW, SHEEHY TL et al. At the bench: Engineering the next generation of cancer vaccines. J Leukoc Biol 2020; 108: 1435–1453. https://doi.org/10.1002/JLB.5BT0119-016R
[30] BAXEVANIS CN, FORTIS SP, ARDAVANIS A, PEREZ SA. Exploring Essential Issues for Improving Therapeutic Cancer Vaccine Trial Design. Cancers 2020; 12: 2908. https://doi.org/10.3390/cancers12102908
[31] DUHEN R, BALLESTEROS-MERINO C, FRYE AK, TRAN E, RAJAMANICKAM V et al. Neoadjuvant anti-OX40 (MEDI6469) therapy in patients with head and neck squamous cell carcinoma activates and expands antigen-specific tumor-infiltrating T cells. Nat Commun 2021; 12: 1047. https://doi.org/10.1038/s41467-021-21383-1
[32] KUANG Z, JING H, WU Z, WANG J, LI Y et al. Development and characterization of a novel anti-OX40 antibody for potent immune activation. Cancer Immunol Immunother 2020; 69: 939–950. https://doi.org/10.1007/s00262-020-02501-2
[33] SCHERWITZL I, OPP S, HURTADO AM, PAMPENO C, LOOMIS C et al. Sindbis Virus with Anti-OX40 Overcomes the Immunosuppressive Tumor Microenvironment of Low-Immunogenic Tumors. Mol Ther Oncolytics 2020; 17: 431–447. https://doi.org/10.1016/j.omto.2020.04.012
[34] FU Y, LIN Q, ZHANG Z, ZHANG L. Therapeutic strategies for the costimulatory molecule OX40 in T-cell-mediated immunity. Acta Pharm Sin B 2020; 10: 414–433. https://doi.org/10.1016/j.apsb.2019.08.010
[35] KISHTON RJ, LYNN RC, RESTIFO NP. Strength in Numbers: Identifying Neoantigen Targets for Cancer Immunotherapy. Cell 2020; 183: 591–593. https://doi.org/10.1016/j.cell.2020.10.011
[36] WELLS DK, VAN BUUREN MM, DANG KK, HUBBARD-LUCEY VM, SHEEHAN KCF et al. Key Parameters of Tumor Epitope Immunogenicity Revealed Through a Consortium Approach Improve Neoantigen Prediction. Cell 2020; 183: 818–834. https://doi.org/10.1016/j.cell.2020.09.015

https://doi.org/10.4149/neo_2023_230125N41

Tumor-derived autophagosome vaccines combined with immune adjuvants mediate antitumor immune responses via the neoantigen pathway

Jia YUAN[1], Yue CHANG[2], Yalan DAI[2], Yutong CHEN[2], Rongbin YUE[3], Linjuan ZENG[2,*]

Supplementary Information

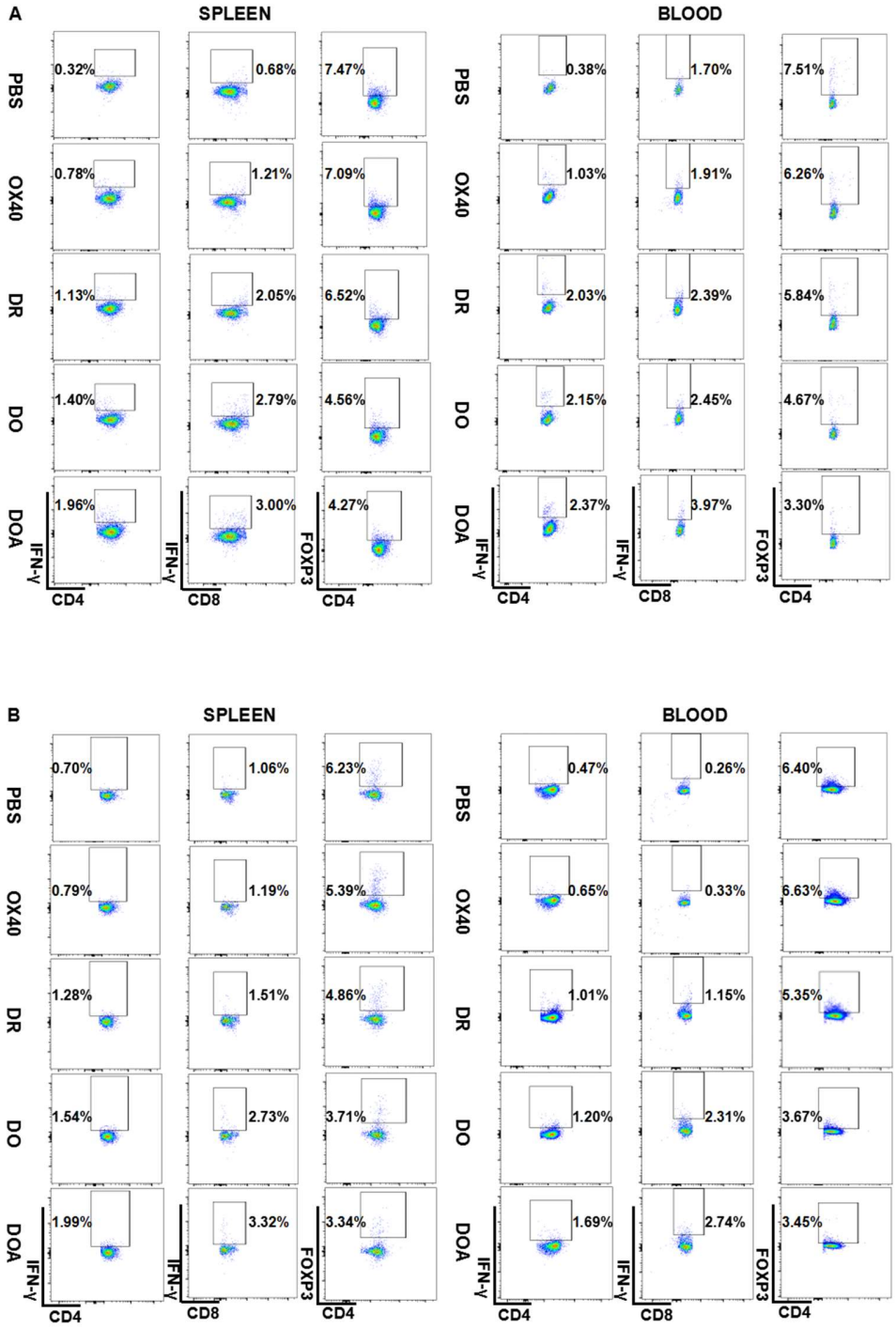

Supplementary Figure S1. Immunological analysis of the systemic effects of treatment with DRibbles, anti-OX40 antibody and ATP. A) Detailed information of flow cytometry for the percentages of IFN-γ-producing CD4+ T cells, CD8+ T cells, and FoxP3+ T cells on day 15 in spleen (left panel) and peripheral blood (right panel) samples from mice with B16F10 tumors treated with PBS, OX40, DR, DO, and DOA. B) Flow cytometry analysis of the percentages of IFN-γ-producing CD4+ T cells, CD8+ T cells, and FoxP3+ T cells on day 20 in spleen (left panel) and peripheral blood (right panel) samples from mice with 4T1 tumors treated with PBS, OX40, DR, DO, and DOA. DR, DRibbles; DO, DR+OX40; DOA, DR+OX40+ATP.

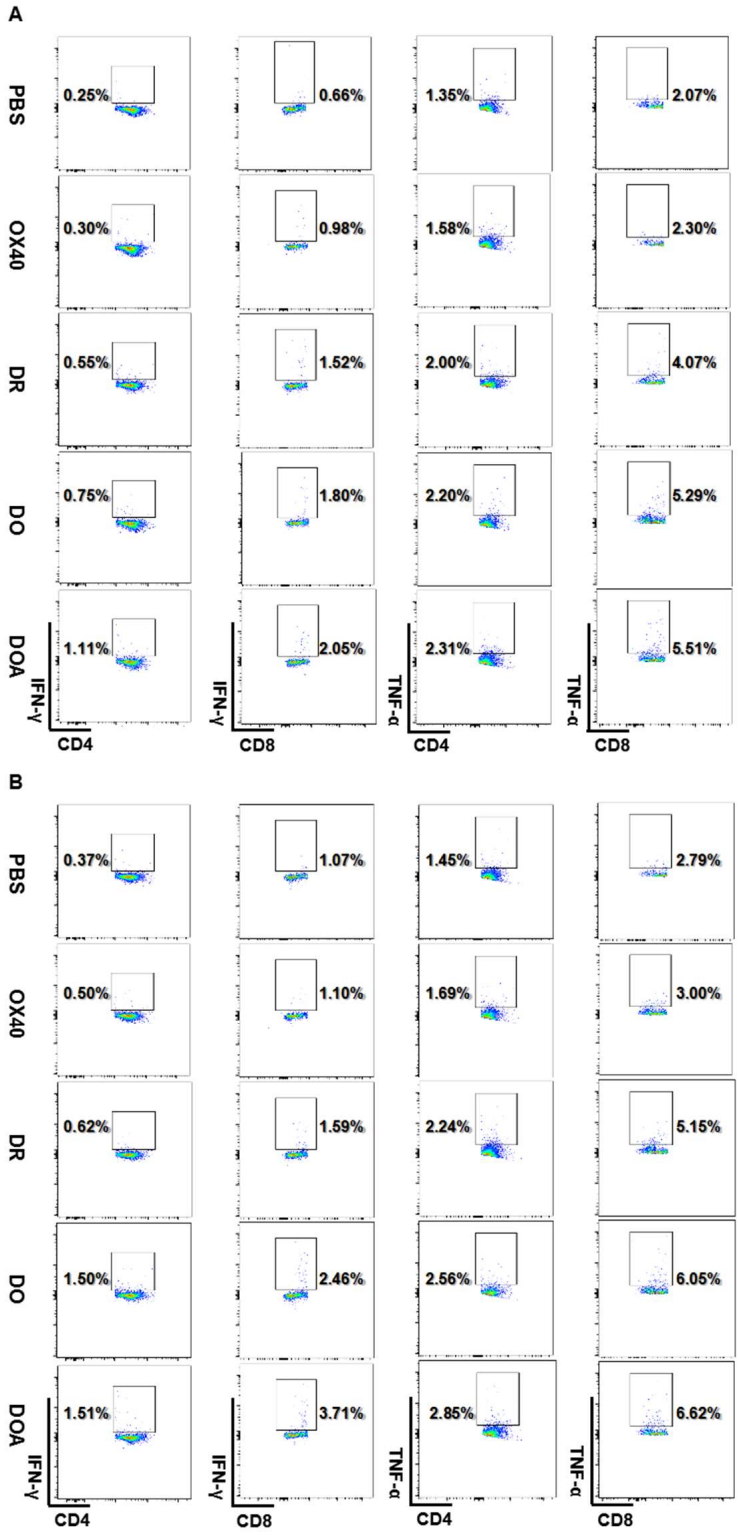

Supplementary Figure S2. Induction of tumor-reactive T cells by DRibbles treatment. A, B) Detailed information of flow cytometry for intracellular cytokine (IFN-γ and TNF-α) secretion. Through CD4/CD8 surface and intracellular cytokine (IFN-γ and TNF-α) staining, flow cytometry was performed to analyze the activation of splenic T cells incubated with B16F10 tumor cells in different groups (PBS, OX40, DR, DO, and DOA). C, D) Detailed information of flow cytometry for intracellular cytokine (IFN-γ and TNF-α) secretion. Through CD4/CD8 surface and intracellular cytokine (IFN-γ and TNF-α) staining, flow cytometry was performed to analyze the activation of splenic T cells incubated with 4T1 tumor cells in different groups (PBS, OX40, DR, DO, and DOA).

A

Mutation	Gene	Mutated sequence used for text	Substitution (WT, AA#, Mut)
B16-M-	-	NVSPELNSTDQP	-
B16-M27	Obsl1	REGVELCPGNKYEMRRHGTTHSLVIHD	T1764M
B16-M30	Kif18b	PSKPSFQEFVDWENVSPELNSTDQPFL	K739N

B

Mutation	Gene	Mutated sequence used for text	Substitution (WT, AA#, Mut)
4T1-M-	-	LAAQSLGEPATQITLNTFHYAGVSAKN	-
4T1-M8	Tmtc2	QGVTVLAVSAVYDIFVFHRLKMKQILP	V201I
4T1-M17	Malt1	FLKDRLLEDKKIAVLLDEVAEDMGKCH	T534A

C

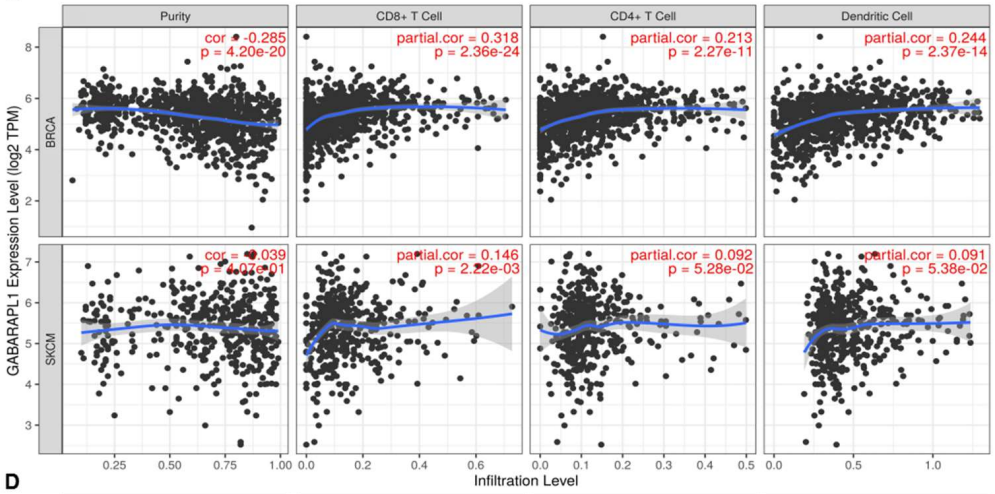

D

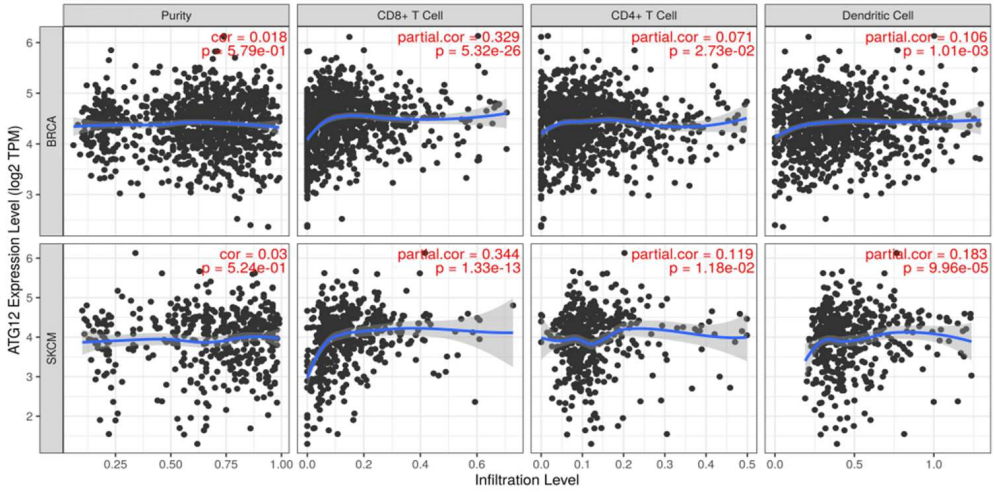

Supplementary Figure S3. Detailed information about the B16F10/4T1-associated neoantigen peptides and related bioinformatic analysis in BRCA and SKCM patients. A, B) Tables showed the details of the synthesis of the optimal B16F10-associated (A) and 4T1-associated (B) neoantigen peptides. C, D) Correlations between the expression levels of ATG8 (GABAPARAPL1) (C) and ATG12 (D) and the abundances of CD8 + T cells, CD4 + T cells, and DCs in BRCA (upper panel) and SKCM (lower panel) tissues. BRCA, breast invasive carcinoma; SKCM, skin cutaneous melanoma.

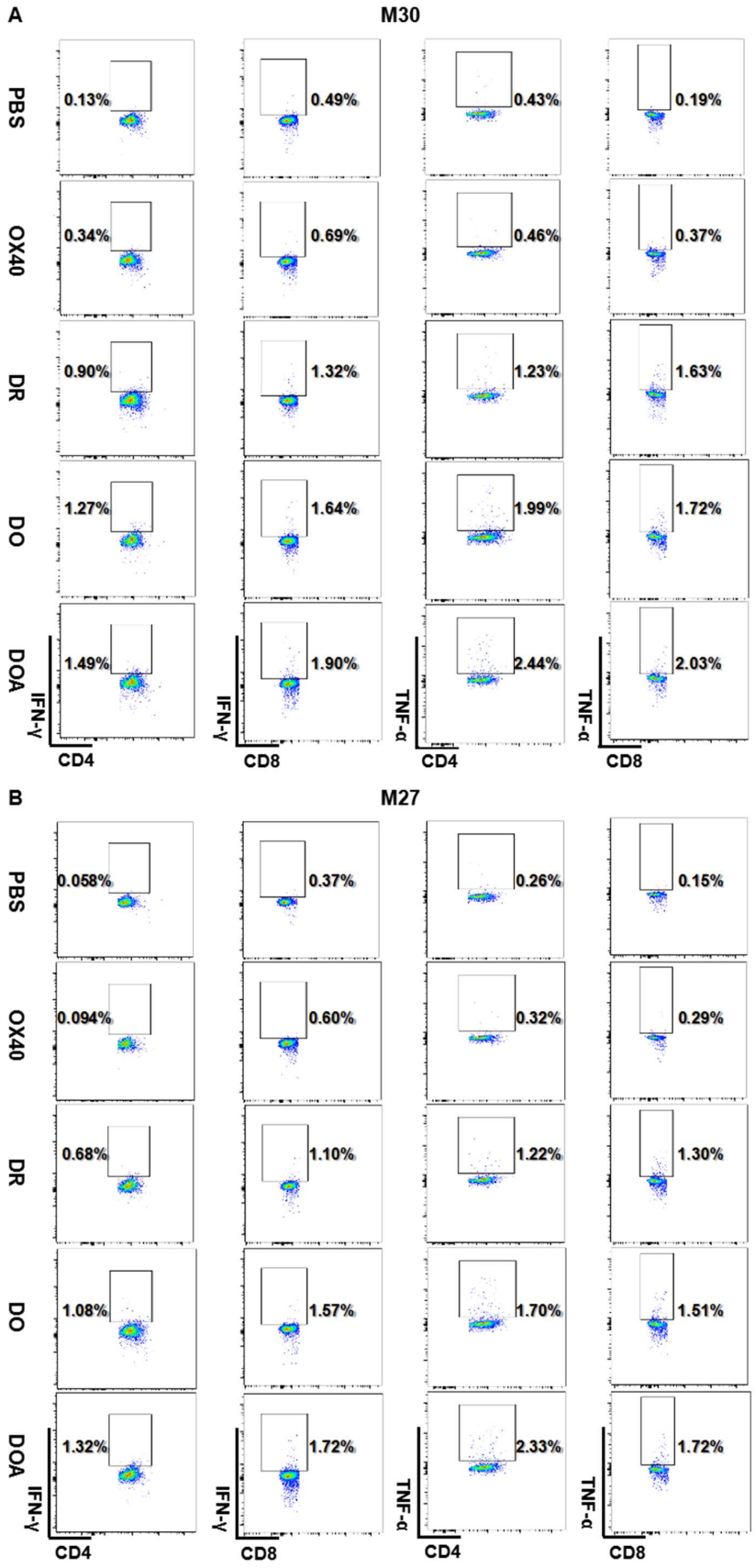

Supplementary Figure S4. Detailed information of B16F10/4T1-associated neoantigen peptides related immunogenicity testing. A, B) Flow cytometry for Intracellular cytokine (IFN-γ and TNF-α) secretion in neoantigen specific T cell immune responses of B16F10 model. Through CD4/CD8 surface and intracellular cytokine IFN-γ/TNF-α staining, flow cytometry was performed to analyze the activation of splenic T cells incubated with neoantigen peptides (M30 and M27). C, D) Flow cytometry for Intracellular cytokine (IFN-γ and TNF-α) secretion in neoantigen specific T cell immune responses of 4T1 model. Through CD4/CD8 surface and intracellular cytokine IFN-γ/TNF-α staining, flow cytometry was performed to analyze the activation of splenic T cells incubated with neoantigen peptides (M8 and M17).